Pharm Res (2017) 34:1402–1415
DOI 10.1007/s11095-017-2157-8

RESEARCH PAPER

Breast Cancer Resistance Protein and Multidrug Resistance Protein 2 Regulate the Disposition of Acacetin Glucuronides

Huangyu Jiang[1] • Jia Yu[1] • Haihui Zheng[1] • Jiamei Chen[1] • Jinjun Wu[1] • Xiaoxiao Qi[1] • Ying Wang[1] • Xinchun Wang[2] • Ming Hu[1,3] • Lijun Zhu[1] • Zhongqiu Liu[1,4]

Received: 27 December 2016 / Accepted: 31 March 2017 / Published online: 18 April 2017
© Springer Science+Business Media New York 2017

ABSTRACT

Purpose To determine the mechanism responsible for acacetin glucuronide transport and the bioavailability of acacetin.

Methods Area under the curve (AUC), clearance (CL), half-life ($T_{1/2}$) and other pharmacokinetic parameters were determined by the pharmacokinetic model. The excretion of acacetin glucuronides was evaluated by the mouse intestinal perfusion model and the Caco-2 cell model.

Results In pharmacokinetic studies, the bioavailability of acacetin in FVB mice was 1.3%. Acacetin was mostly exposed as acacetin glucuronides in plasma. AUC of acacetin-7-glucuronide (Aca-7-Glu) was 2-fold and 6-fold higher in Bcrp1 (−/−) mice and Mrp2 (−/−) mice, respectively. AUC of acacetin-5-glucuronide (Aca-5-Glu) was 2-fold higher in Bcrp1 (−/−) mice. In mouse intestinal perfusion, the excretion of Aca-7-Glu was decreased by 1-fold and 2-fold in Bcrp1 (−/−) and Mrp2 (−/−) mice, respectively. In Caco-2 cells, the efflux rates of Aca-7-Glu and Aca-5-Glu were significantly decreased by breast cancer resistance protein (BCRP) inhibitor Ko143 and multidrug resistance protein 2 (MRP2) inhibitor LTC4. The use of these inhibitors markedly increased the intracellular acacetin glucuronide content.

Conclusions BCRP and MRP2 regulated the *in vivo* disposition of acacetin glucuronides. The coupling of glucuronidation and efflux transport was probably the primary reason for the low bioavailability of acacetin.

KEY WORDS acacetin · bioavailability · efflux transporter · excretion · pharmacokinetic

ABBREVIATIONS

AP	Apical
AUC	Area under the curve
BCRP	Breast cancer resistance protein
BL	Basolateral
C_{max}	Maximum plasma concentration
CL	Clearance
HBSS	Hanks' balanced salts
HPLC	High performance liquid chromatography
HRMS	High-resolution mass spectra
LLOQ	Lower limit of quantification
MRP	Multidrug resistance protein
MRT	Mean residence time
$T_{1/2}$	Half-life
UGT	Uridine 5′-diphospho-glucuronosyltransferases
UHPLC-MS/MS	Ultra high performance liquid chromatography/tandem mass spectrometry
UV	Ultraviolet and visible spectrum

INTRODUCTION

Flavonoids are a class of polyphenolic natural compounds that have been extensively investigated because of their diverse health benefits. This series of compounds occurs naturally as

✉ Lijun Zhu
zhulijun@gzucm.edu.cn

✉ Zhongqiu Liu
liuzq@gzucm.edu.cn

[1] International Institute for Translational Chinese Medicine Guangzhou University of Chinese Medicine Guangzhou, Guangdong 510006, China

[2] First Affiliated Hospital of the Medical College Shihezi University Shihezi 832008, China

[3] Department of Pharmacological and Pharmaceutical Sciences College of Pharmacy University of Houston Houston, Texas 77030, USA

[4] State Key Laboratory of Quality Research in Chinese Medicine Macau University of Science and Technology Macau (SAR), China

glucosides and aglycones in medicinal plants and herbal remedies. In general, flavonoids, such as genestein, possess low oral bioavailability because they can easily undergo conjugating reactions catalyzed by phase II enzymes including UDP-glucuronosyltransferases (UGTs) and sulfotransferases (1,2). The excretion of the generated metabolites requires the efflux transporters because these metabolites are highly hydrophilic. According to published researches, breast cancer resistance protein (BCRP), multidrug resistance protein 2 (MRP2) and MRP3 can transport numerous glucuronide conjugates (3–6). However, these efflux transporters exhibit substrate selectivity in the transport of these metabolites. For instance, quercetin glucuronide is transported by Bcrp but not by Mrp2 (7). BCRP rather than MRP2 plays an important role in the biliary excretion of mycophenolic acid glucuronide. MRP2 facilitates the biliary excretion of the glucuronide conjugate of methyl-1(3,4-dimethoxyphenyl)-3-(3-ethylvaleryl)-4-hydroxy-6,7,8-trimethoxy-2-naphthoate, but the effect of BCRP on this conjugate is limited (8). Because transporters possibly induce drug-drug interactions (DDIs), the roles of efflux transporters should be evaluated to help predict the potential DDIs during drug development (9,10).

Flavone acacetin (5,7-dihydroxy-4′-methoxyflavone) is a bioactive compound distributed in many natural plants such as *Dracocephalum moldavica* L., propolis, *Tunera diffusa and Betula pendula* (11–13). It has been recognized as a highly potential drug candidate because it has a broad spectrum of biological activities. Acacetin can induce apoptosis in T cells associated with leukemia by activating the Fas-mediated pathway (14). Acacetin has potential curative effects for atrial fibrillation by specifically blocking multiple atrial ion channels (15). It also provides promising treatment effects on inflammation and asthma by inhibiting eotaxin-1- and Th2-associated cytokines (16).

Elucidating the *in vivo* disposition of acacetin may help enhance our understanding on the characteristics of acacetin. In our previous study, acacetin can easily undergo *in vitro* UGT metabolism to Aca-7-Glu via human UGT isoforms and different microsomes from humans and other animals, such as mouse, rat, and dog (17). Among human UGT isoforms, UGT1A8 produces the highest number of metabolites (17). *In vivo* pharmacokinetics have demonstrated that Aca-7-Glu showed higher plasma level than that of acacetin (18). After 200 or 400 mg/kg of *D. moldavica* L. mixture is orally administered to Sprague–Dawley rats, AUC of Aca-7-Glu is extremely higher (>26-fold) than that of acacetin (18). Acacetin and its glucoside tilianin may participate in a triple recycling process consisting of enterohepatic recycling, enteric recycling, and local recycling, which are facilitated by the coupling of UGTs and efflux transporters (19). Thus, all of the evidences suggested that extensive UDP-glucuronosyltransferase (UGT) metabolism may contribute signficantly to the poor bioavailability of acacetin. The excretion of most UGT metabolites are mediated by efflux transporters (e.g., BCRP and MRP2). Therefore, our current study was designed to elucidate the roles of apical efflux transporters involved in acacetin glucuronide transport. In addition, the bioavailability of acacetin remains unknown.

In this study, a sensitive and stable UHPLC-MS/MS method was initially established. Comprehensive and thorough *in vivo* analyses were subsequently conducted to determine the bioavailability of acacetin and understand its disposition. The established method could be used to quantify acacetin and its glucuronides, namely, Aca-5-Glu and Aca-7-Glu. The bioavailability of acacetin was observed in FVB mice. In the pharmacokinetic analysis of acacetin glucuronides, knockout mice were utilized to reveal the effects of efflux transport on their systemic exposure levels. Knockout mice used in the perfusion model and Caco-2 cells with chemical inhibitors were combined to confirm the roles of transporters in the excretion of acacetin glucuronides.

MATERIALS AND METHODS

Materials

Cloned Caco-2 cells (TC7) were kindly provided by Dr. Ming Hu (Department of Pharmaceutical Sciences, College of Pharmacy, University of Houston, USA). HPLC-grade acacetin (purity ≥98%, confirmed through UHPLC-MS/MS) was purchased from Shanghai Winherb Medical Technology Co., Ltd. (Shanghai, China). Testosterone (purity ≥98%; used as an internal standard) was procured from Nacalai Tesque Company (Tokyo, Japan). Leukotriene C4 (LTC4), Ko143, fetal bovine serum, and Hanks' balanced salts (HBSS, powder form) are all bought from Sigma-Aldrich Co. (St. Louis, MO, USA). All other chemicals and solvents were of analytical grade or higher and used as received.

Animals

Eight- to eleven-week-old male wild-type FVB mice were purchased from Vital River Laboratory Animal Technology Co., Ltd. (Beijing, China) and male knockout FVB mice including Mrp2 (−/−) and Bcrp1 (−/−), of the same age were purchased from Biomodel Organism Science & Technology Development Co., Ltd. (Shanghai, China). These mice were maintained in a unidirectional airflow room under the following conditions: relative humidity (40% to 70%), controlled temperature (20 °C to 24 °C) and 12 h/12 h light/dark cycle. These mice weighing 20 g to 30 g were fasted overnight and provided drinking water 1 day before the experiments were performed. Animal experiments were carried out in accordance with mandatory guidelines and approved by the Guangzhou University of Chinese Medicine's Ethics Committee.

Biosynthesis of Aca-7-Glu and Aca-5-Glu

The phase II metabolites Aca-7-Glu and Aca-5-Glu were prepared using rat liver microsomes in accordance with a previously published method (18). Aca-7-Glu and Aca-5-Glu in the preparation solution were seperated with an Agilent 1200 HPLC system (Agilent Technologies, Inc., Santa Clara, CA, USA). The collected solution was concentrated in nitrogen and stored at −20 °C. The concentrations of Aca-7-Glu and Aca-5-Glu were determined on the basis of the standard curve and conversion factor of acacetin. This factor was calculated by comparing the peak area change in aglycone after hydrolyzing glucuronide with β-glucuronidases and the corresponding peak area change in glucuronide under the same UV detection wavelength. The conversion factors of Aca-7-Glu and Aca-5-Glu were 1.2 and 1.4, respectively.

Pharmacokinetic Studies

For pharmacokinetic studies, acacetin was dissolved in ethanol and then diluted in 25% cyclodextrin (1:19, *v*/*v*) for pharmacokinetic studies. For oral (p.o.) administration, FVB mice and knockout mice received 5 mg/kg of acacetin. For intravenous (i.v.) administration, only FVB mice were treated with 0.5 mg/kg of acacetin. Blood samples (approximately 20 μL) were collected by snipping the mouse tail near its tip at 3, 5, 10, 15, 20, 30, 60, 120, 300, 420, 540, and 720 min post-treatment and placed in heparinized tubes. The samples were centrifuged at 8000 rpm for 8 min. Afterward, plasma was obtained and stored at −20 °C until analysis. Plasma samples were prepared as follows: 10 μL of sample was spiked with 60 μL of methanol to precipitate protein, and the mixture was vortexed for 1 min. The sample was then centrifuged at 14,000 rpm for 15 min, and 60 μL of the supernatants was transferred to a new tube and evaporated to dryness in a vacuum drying oven. The residue was dissolved with 60 μL of 50% methanol aqueous solution, centrifuged at 13,500 rpm for 30 min, and analyzed by using a UHPLC-MS/MS system. The pharmacokinetic parameters were identified with WinNonlin 3.3 (Pharsight Co., Mountain View, CA, USA). The absolute oral bioavailability (F%) of acacetin was calculated by using the following equation:

$$\mathrm{F}\% = \frac{AUC(p.o.) \times \mathrm{Dose}(i.v.)}{AUC(i.v.) \times \mathrm{Dose}(p.o.)} \times 100\%$$

Studies on Liver Distribution

The method to dissolve acacetin was the same as pharmacokinetic studies. Mice (FVB, Bcrp1(−/−) and Mrp2 (−/−) mice) were drawn blood from eye ball and were sacrificed 5 min following oral administration of 5 mg/kg acacetin. They were then immediately transferred to a tray after removing the liver from the animals. The liver was washed with saline until the external blood was completely removed from the organ. Pieces of 1000–1500 mg of the liver were taken and washed again, blotted with filter paper, and weighed. They were firstly chopped with blade and 1000 μL saline was added per 1000 mg of tissue, followed by homogenising for approximately 3 min at 60 Hz in an automatic grinding machine. The sample was stored at −20 °C until analysis. Samples of liver tissue and plasma were prepared similar to pharmacokinetic studies as the following: 20 μL of sample was spiked with 80 μL of methanol to precipitate protein, and the mixture was vortexed for 1 min. The sample was then centrifuged at 14,000 rpm for 15 min, and 80 μL of the supernatants was transferred to a new tube and evaporated to dryness in a vacuum drying oven. The residue was dissolved with 80 μL of 50% methanol aqueous solution, centrifuged at 13,500 rpm for 30 min, and analyzed by a UHPLC-MS/MS system.

Transport Experiments in the Perfused Mouse Model

Animal surgery was performed in accordance with a previously described method (20). In brief, after the mouse was anesthetized by 1 g/kg urethane (50%, *w*/*v*), one segment of the small intestine (10 cm) and the colon (7 cm) were simultaneously perfused with HBSS solution containing 5 μM of acacetin at a flow rate of 0.25 mL/min to initiate the experiment. Tween 80 (0.1%, *v*/*v*) and polyethylene glycol 400 (0.2%, *v*/*v*) were added to promote the solubility of acacetin in HBSS buffer (pH 6.5) because we found that acacetin yielded poor solubility at pH 6.5. The intestines were perfused for 20 min to achieve steady-state absorption, and 2 perfusion samples were obtained from the outlet cannula every 20 min. The bile duct was tied before the intestine, and bile was allowed to accumulate inside the gallblader before and during the perfusion. For the perfusate sample, a stop solution (2 mL of ethanol) was added to the receiving tubes to prevent substrate hydrolysis. Tubes used to hold perfusate and bile were weighed before and after accumulation to measure the amount of the collected perfusate and bile. At the end of the experiment, bile samples were collected by tying the liver side of the bile duct and carefully removing the gallbladder with scissors. Blood samples were also collected from the tip of the tail. All inlet cannulas were insulated and maintained at 37 °C by a circulating water bath to ensure that the temperature of the perfusate remained constant. The concentrations of test compounds in the perfusate were analyzed through UHPLC-MS/MS.

Glucuronidation of Acacetin by Mouse S9 Fraction

This procedure was performed in accordance with a previously described protocol (21). Acacetin was incubated with the mouse S9 fraction of the liver or small intestine from FVB mice and knockout mice (i.e., Bcrp1 (−/−) and Mrp2 (−/−) mice) in a UGT incubation system. The protein concentration of this fraction was 0.25 mg/mL.

Metabolism of Acacetin in Caco-2 Cell Lysate

Caco-2 cell lysate was prepared in accordance with a previously described method (21).

Transport Experiments of Acacetin in the Caco-2 Cell Model

Transport experiments were conducted in accordance with published protocols (22). In brief, cell monolayers were washed thrice with HBSS (pH 7.4) at 37 °C. Their transepithelial electrical resistance (Millicell-ERS) was measured, and values less than 460 Ω/cm^2 were discarded. The monolayers with the desired transepithelial electrical resistance were incubated with HBSS for 1 h. Acacetin solution (10 μM) was loaded on either apical (AP) or basolateral (BL) side, and blank HBSS was loaded on the other side. Efflux transporter inhibitors, namely, Ko143 (an inhibitor of BCRP, 10 μM) and LTC4 (an inhibitor of MRP2, 0.1 μM) were added onto the AP side, and each sample was prepared in triplicate. The samples (0.5 mL) were collected at different time points (0, 1, 2, 3, and 4 h), and the same volume of the corresponding solution was used to replenish each well after sampling was conducted. The intracellular concentrations of acacetin glucuronides were determined after transport experiments were performed. Briefly, the cells were removed from the inserts, pooled in blank HBSS (1 mL), and sonicated for 30 min in an ice bath (4 °C). F_{met} was calculated according to a published method (23) as follow:

$$F_{met} = \frac{\sum \text{Metabolite}}{\sum \text{Metabolite} + \sum \text{Acacetin}}$$

Where $\sum$*Metabolite* represents the total concentrations of metabolites, and $\sum$ *Acacetin* is the total concentrations of acacetin combined in the cell, apical and basolateral side. All of the samples were centrifuged at 13,000 rpm for 30 min before measurement was carried out through UHPLC-MS/MS.

UHPLC-MS/MS Analysis of Acacetin and Glucuronides

UHPLC-MS/MS was performed using an Agilent 1290 series UHPLC system with a G4220B binary pump, a G1316C column oven, a G4226A autosampler, and a G4212A DAD (Agilent, USA) and an Agilent 6460 Triple Quadrupole mass spectrometer equipped with an electrospray ionization source (Agilent Technologies). Chromatographic separation was completed by using the UHPLC system. The compounds were analyzed under the following UHPLC conditions: Agilent 1290 infinity LC system; column, ZORBAX SB-C18, 1.8 μm, 3.0 mm × 100 mm; mobile phase A, 100% aqueous buffer (0.1%, *v*/*v* formic acid, pH 2.5); mobile phase B, 100% acetonitrile; flow rate, 0.3 mL/min; mobile phase gradient, 80% A for 0–1.0 min, 85%–70% A for 1.0–2.0 min, 70%–60% A for 2.0–4.0 min, 60%–20% A for 4.0–6.0 min, 20%–85% A for 6.0–8.5 min; detection wavelengths, 330 and 254 nm; and injection volume, 10 μL.

MS/MS was applied to verify the structure of the compounds, multiple reaction monitoring (MRM) was performed to analyze the compounds quantitatively. The relevant parameters of the mass spectrum were as follows: fragmentor, 135 kV; nozzle voltage, 500 V; gas temperature, 280 °C; sheath gas temperature, 380 °C; and sheath gas flow, 7.0 L/min. For the first 2 min, the samples were diverted to the waste, and from 2 to 8.5 min, the samples were switched into the mass spectrometer for analysis. The following transitions were obtained: m/z 461.0 > 285.1 for Aca-7-Glu and Aca-5-Glu, m/z 285.2 > 241.9 for acacetin, and m/z 289.0 > 97.1 for testosterone (internal standard, IS). The lower limits of quantification (LLOQ) were 0.2 and 2 nM for acacetin glucuronides and acacetin, respectively.

Statistical Analysis

Data were presented as means ± standard deviation. One-way ANOVA with or without Turkey–Kramer's multiple comparison or student's *t* test was used to evaluate statistical differences. Differences were considered significant at $p < 0.05$.

RESULTS

Identification of Acacetin and Acacetin Glucuronides

After acacetin was incubated with rat liver microsomes, two distinct peaks of the absorbances G1 and G2 with different retention times (4.5 min for Aca-5-Glu and 5.0 min for Aca-7-Glu) were identified in the diode array detector (Fig. 1a). Both compounds showed pseudo-molecule ion $[M + H]^+$ of m/z 461.000 in the full scan mass spectra. These findings suggested that the molecular formula of these compounds

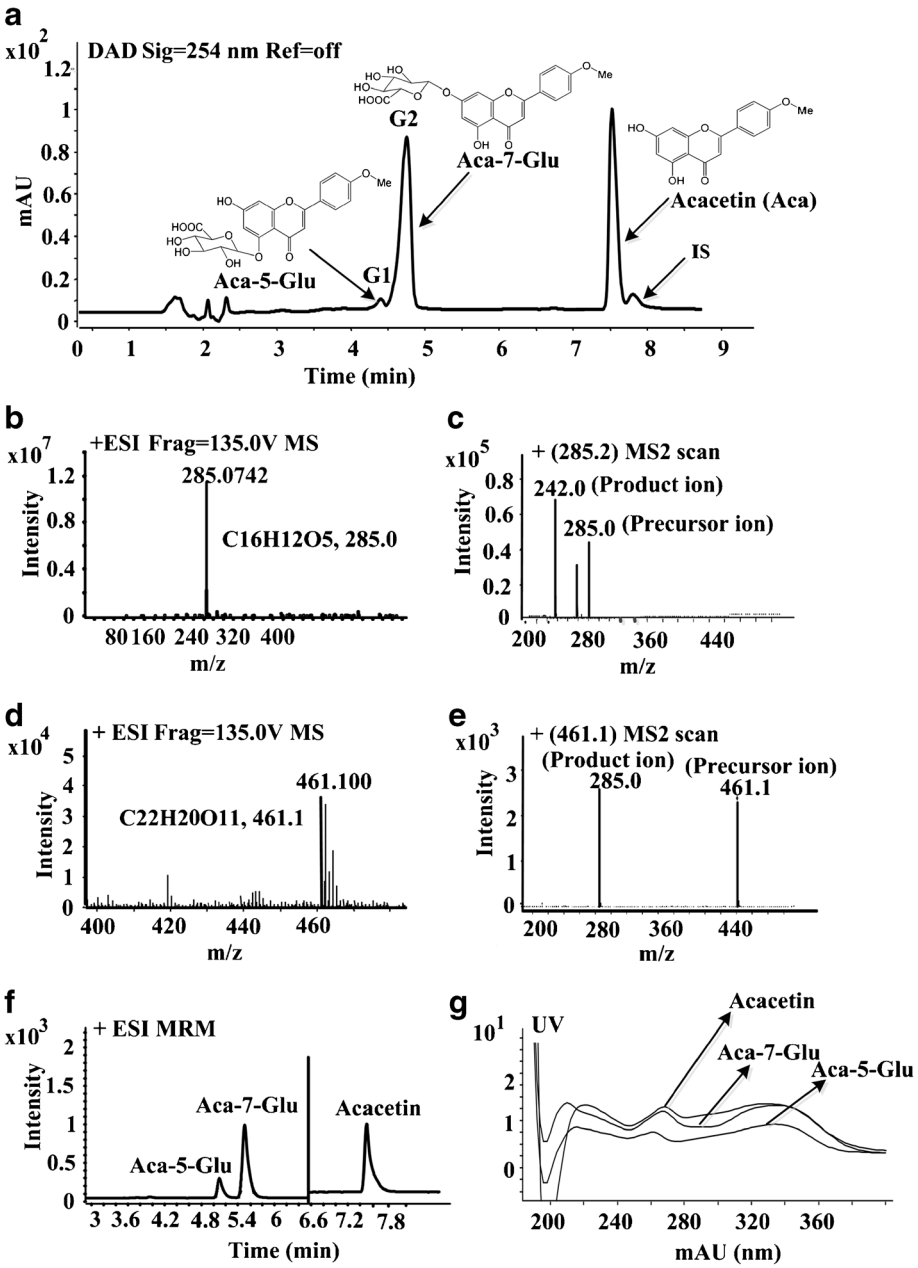

Fig. 1 Representative UHPLC-DAD (**a**, **g**), UHPLC-MS/MS (**b**-**f**) chromatograms of acacetin, acacetin-5-glucuronide (Aca-5-Glu) and acacetin-7-glucuronide (Aca-7-Glu) and their respective structures. Panel (**a**) shows DAD chromatogram of acacetin, Aca-7-Glu and Aca-5-Glu and internal standard (IS). Panels (**b**) and (**d**) show high-resolution mass spectra of acacetin and acacetin glucuronides, respectively. Panels (**c**) and (**e**) show the MS2 scan for acacetin and acacetin glucuronides, respectively. Panel (**f**) represents the MRM chromatograms of acacetin and acacetin glucuronides. Panel (**g**) shows UV spectra of acacetin and acacetin glucuronides. UHPLC was used to separate acacetin and its glucuronides and MRM method was used for quantification of each compound. The MS2 scan was used for confirming their identities. UV spectra (**g**) was used to distinguish Aca-7-Glu and Aca-5-Glu.

was $C_{22}H_{20}O_{11}$ (Fig. 1d). In the MS2 scan, a precursor ion of *m/z* 461.0 and a product ion of *m/z* 285.0 were observed in these compounds (Fig. 1e), and these ions corresponded to acacetin glucuronides. The high-resolution mass spectra of these compounds showing $[M + H]^+ = 285.0742$ ion indicated that their molecular formula was $C_{16}H_{12}O_5$ (Fig. 1b). The MS2 scan displaying a precursor ion of *m/z* 285.0 and a product ion of *m/z* 242.0 confirmed the structure of acacetin (Fig. 1c).

UV spectra method can be applied to distinguish acacetin glucuronides (24). Flavones including their glucuronides, yield two major absorption peaks ranging from 240 nm to 280 nm, which is commonly referred to as band II, and ranging from 300 nm to 380 nm, which is commonly referred to as band I. Monoglucuronidated 5-hydroxyl group resulted in a band II λ_{max} hypsochromic shift whereas monoglucuronidated 7-hydroxyl group caused little change in λ_{max}. The UV spectra of acacetin and the generated glucuronides are shown in Fig. 1a and g. In Fig. 1g, the λ_{max1} and λ_{max2} of acacetin were located in approximately 270 and 330 nm, respectively. Compared with that of acacetin, the UV spectrum with 10 nm hypsochromic shifts at λ_{max1} was identified as Aca-5-Glu, whereas the UV spectrum without any changes in λ_{max1} was determined as Aca-7-Glu. The UHPLC retention time and the acacetin glucuronides identified are summarized in Table I.

Table I Retention Time of Acacetin and Its Glucuronides in UHPLC Chromatograms with the HRMS Data as Well as Their Respective UV Spectral Data

Compound	UHPLC t_R (min)	$[M + H]^+$ (m/z)	Molecular formula	Band I max (nm)	Band II max (nm)	Shift in bands I and II (nm)	Identification
Acacetin	7.3	285.2072	$C_{16}H_{12}O_5$	338	266	–	–
G1	4.5	461.1000	$C_{22}H_{20}O_{11}$	336	260	– 6 (Band II)	acacetin-5-glucuronide
G2	5.0	461.1067	$C_{22}H_{20}O_{11}$	338	266	no change	acacetin-7-glucuronide

Pharmacokinetic Characteristics of Acacetin in Mice

Pharmacokinetic Characteristics of Acacetin, Aca-7-Glu and Aca-5-Glu in FVB Mice

After acacetin was intravenously or orally administered to FVB mice, the concentrations of acacetin, Aca-7-Glu and Aca-5-Glu were determined and their mean plasma concentration-time curves are shown in Fig. 2. The corresponding pharmacokinetic parameters are listed in Table II. The absolute bioavailability of acacetin obtained from the FVB mice was 1.3%. Once orally administered, acacetin was quickly absorbed and metabolized into Aca-7-Glu and Aca-5-Glu (Table II). The maximum plasma concentration (C_{max}) of Aca-7-Glu was 5-fold higher than that of acacetin. The CL of Aca-7-Glu and Aca-5-Glu was 24-fold and approximately 3-fold lower than that of acacetin, respectively. The $T_{1/2}$ and mean residence time (MRT) of these glucuronides were shorter than those of acacetin. After acacetin was intravenously administered, considerable amounts of Aca-7-Glu could be measured (Fig. 2b). By comparison, the amounts of Aca-5-Glu were under LLOQ 30 min after acacetin was administered (Fig. 2c). $AUC_{0-\infty}$ and CL of Aca-7-Glu were lower than those of acacetin. The C_{max}, $T_{1/2}$ and MRT of Aca-7-Glu were 2-fold to 3-fold lower than those of acacetin.

Pharmacokinetic Characteristics of Aca-7-Glu and Aca-5-Glu in Knockout Mice and FVB Mice

The mean plasma concentration–time curves of Aca-7-Glu and Aca-5-Glu and their pharmacokinetic parameters following oral acacetin administration (5 mg/kg dose) for the analysis of transporter knockout mice are shown in Fig. 3. For Aca-7-Glu, $AUC_{0-\infty}$ was 2- and 6-fold higher when Bcrp or Mrp2 expressed in the AP membrane was knocked out ($p < 0.05$) (Fig. 3c1), whereas CL was significantly reduced ($p < 0.05$) (Fig. 3c2). $T_{1/2}$ was significantly lower in the absence of Mrp2 ($p < 0.05$) than that in FVB mice (Fig. 3c3). By contrast, $T_{1/2}$ did not significantly change in the absence of Bcrp. For Aca-5-Glu, $AUC_{0-\infty}$ in Bcrp1 (−/−) mice, which lacked a Bcrp transporter expressed in the AP membrane of liver, intestine, breast and kidney, was 2-fold to 3-fold higher than that in FVB mice ($p < 0.05$). CL and $T_{1/2}$ of

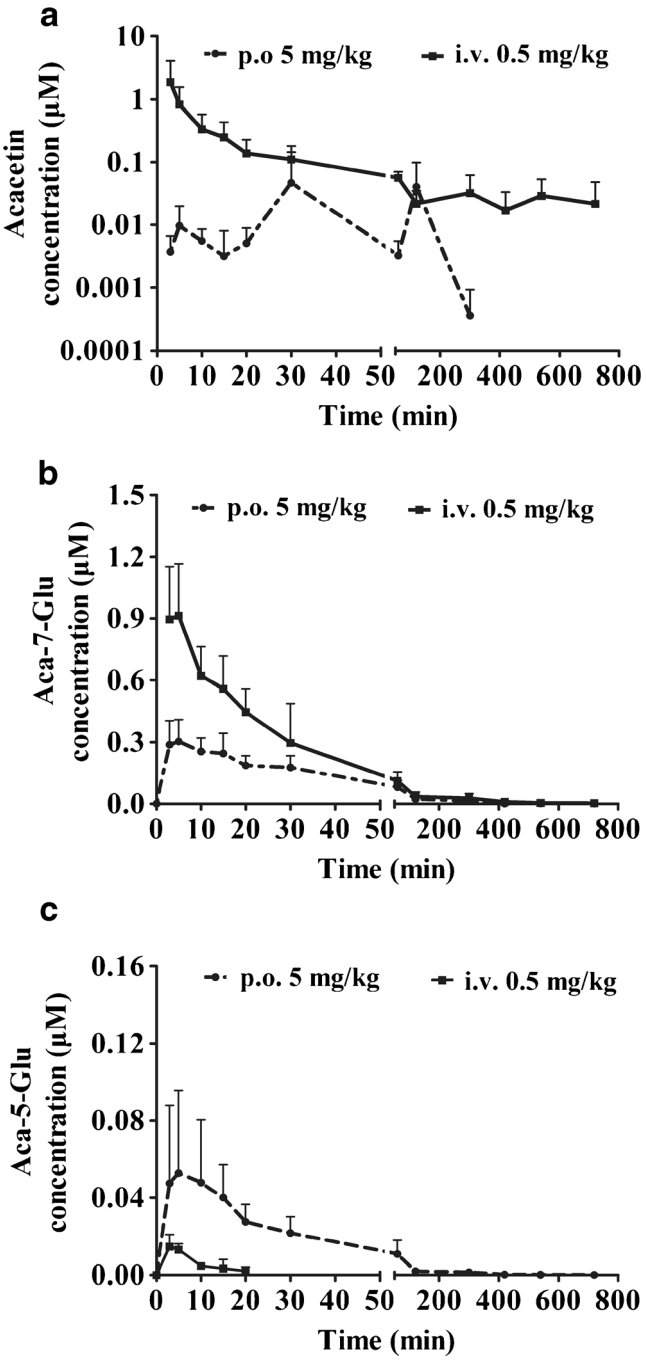

Fig. 2 Concentration-time curves of plasma concentrations of acacetin (**a**) Aca-7-Glu (**b**) and Aca-5-Glu (**c**) following oral (5 mg/kg) and intravenous (0.5 mg/kg) administration of acacetin in FVB mice ($n = 5$).

Table II Pharmacokinetic Parameters of Acacetin, acacetin-7-glucuronide (Aca-7-Glu) and acacetin-5-glucuronide (Aca-5-Glu) Following Oral (5 mg/kg) and Intravenous (0.5 mg/kg) Administration of Acacetin (Aca) in FVB Mice

Compound	Dose and route	C_{max} (μmol/L)	$AUC_{0-\infty}$ (min•μmol/L)	CL (L/min/kg)	$T_{1/2}$ (min)	MRT (min)
Aca	5 mg/kg p.o.	0.06 ± 0.09	6.2 ± 8.7	24 ± 30	81 ± 71	140 ± 87
	0.5 mg/kg i.v.	1.8 ± 2.2	49 ± 41	0.55 ± 0.33	147 ± 59	309 ± 175
Aca-7-Glu	5 mg/kg p.o.	0.32 ± 0.11	18 ± 3.4	1.0 ± 0.22	31 ± 5.8	87 ± 34
	0.5 mg/kg i.v.	1.0 ± 0.28	38 ± 12	0.51 ± 0.18	78 ± 27	102 ± 51
Aca-5-Glu	5 mg/kg p.o.	0.06 ± 0.04	2.3 ± 1.1	9.5 ± 4.8	24 ± 4.6	70 ± 31
	0.5 mg/kg i.v.	N.C.	N.C	N.C	N.C	N.C

Data shown are mean ± standard deviation, $n = 5$

C_{max}, maximum plasma concentration; $AUC_{0-\infty}$, area under the curve extrapolated to infinity; CL, clearance; $T_{1/2}$, half-life; MRT, mean residence time

N.C., not calculated

Aca-5-Glu did not significantly change in Bcrp1 (−/−) and Mrp2 (−/−) mice. The plasma concentrations of acacetin in these knockout mice were fairly low and thus we did not show the result.

Liver Distribution of Acacetin, Aca-7-Glu and Aca-5-Glu in FVB and Knockout Mice

We determined the concentrations of acacetin and its glucuronides in plasma and the liver 5 min after acacetin was orally treated to FVB, Bcrp1 (−/−) and Mrp2 (−/−) mice. Acacetin and Aca-7-Glu could be measured in the liver. In addition to these compounds, a small amounts of Aca-5-Glu could be also determined in plasma. In the liver, Aca-7-Glu showed 4-fold higher concentrations in Mrp2 (−/−) mice compared to FVB mice ($p < 0.05$). In plasma, Aca-7-Glu in Mrp2 (−/−) mice shows markedly higher concentrations (8-fold) ($p < 0.05$). On the contratry, the concentration of acacetin in the liver of FVB mice was 2-fold higher than that in Mrp2 (−/−) mice ($p < 0.05$) but no signicant difference was fould in Bcrp1 (−/−) mice. In plasma, there was no significant difference for acacetin between FVB and knockout mice. More Aca-7-Glu was detected in Bcrp1 (−/−) mice than FVB mice but no statistical difference was observed. Both knockout mice showed more Aca-5-Glu compared to FVB mice in plasma ($p < 0.05$).

Transport Experiments in Mouse Intestinal Perfusion

Bcrp1 (−/−) and Mrp2 (−/−) mice were used to confirm the role of BCRP and MRP2 in glucuronide transport (Fig. 4). Aca-7-Glu was the main glucuronide found in the intestine, bile, or plasma of the tested mice, whereas Aca-5-Glu could not be detected in these samples. The amounts of the excreted Aca-7-Glu were significantly different among the three mouse strains. In particular, the amounts of Aca-7-Glu extruded by the small intestine were remarkably higher than those extruded by the colon (Fig. 4a). The efflux of glucuronide in the small intestine also significantly differed among the mouse strains. Compared with those in the FVB mice, the excreted amounts of glucuronide were 2-fold and 3-fold lower in Bcrp1 (−/−) mice ($p < 0.05$) and Mrp2 (−/−) mice ($p < 0.05$), respectively. The amounts of glucuronide in the colon were rather low, and the glucuronides excreted by the Bcrp1 (−/−) mice were undetectable (Fig. 4a). The amounts of Aca-7-Glu excreted through the bile of the FVB mice were higher than those of the knockout mice, but the difference was not significant, as indicated by a high standard deviation (Fig. 4b). The amounts of Aca-7-Glu observed in plasma were comparable among the mouse strains (Fig. 4c).

Glucuronidation of Acacetin by Mouse S9 Fraction

Aca-7-Glu and Aca-5-Glu were generated when acacetin was incubated with S9 fraction in the small intestine prepared from Bcrp1 (−/−) mice and Mrp2 (−/−) mice, whereas only Aca-7-Glu was found in the liver. In particular, the formation rates of Aca-7-Glu were significantly reduced by the S9 fraction in the liver of Bcrp1 (−/−) mice and Mrp2 (−/−) mice at three concentrations (Fig. 5a) ($p < 0.05$). By comparison, the formation rates of both glucuronides were significantly increased in the small intestine of the knockout mice at 2.5 μM (Fig. 5b, c) ($p < 0.05$). The formation rates of Aca-5-Glu at 40 μM were not shown because it could not be detected in our study.

Metabolism of Acacetin in the Caco-2 Cell Lysate

Acacetin could be metabolized to form Aca-7-Glu and Aca-5-Glu in Caco-2 cell lysate (0.5 mg/mL protein concentration) at 2.5, 10 and 40 μM. The formation rates of both glucuronides increased as the concentration of acacetin increased (Fig. 6). The formation rates of Aca-7-Glu were significantly higher than those of Aca-5-Glu at the three concentrations ($p < 0.05$).

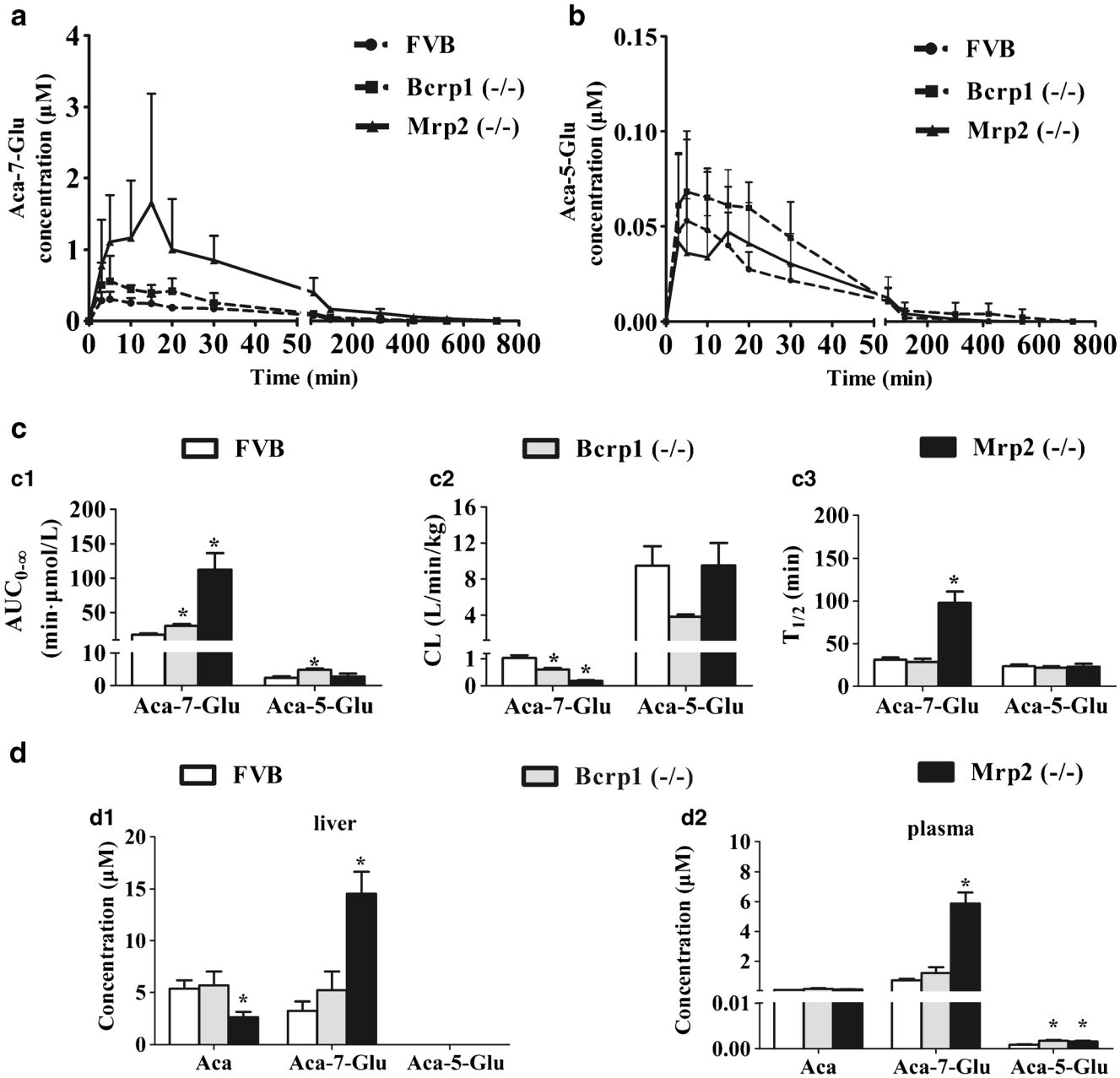

Fig. 3 Concentration-time curves of plasma concentrations of Aca-7-Glu (**a**) and Aca-5-Glu (**b**) along with their pharmacokinetic parameters (**c**) of $AUC_{0-\infty}$ (c 1), CL (c 2) and $T_{1/2}$ (c 3) following oral (5 mg/kg) administration of acacetin in FVB, Bcrp1 (−/−) and Mrp2 (−/−) mice ($n = 5$). Concentrations of acacetin and glucuronides in the liver (d 1) and plasma (d 2) 5 min after acacetin was orally administered to FVB, Bcrp1(−/−) and Mrp2(−/−) mice ($n = 4$). *$p < 0.05$.

Efflux of Acacetin Glucuronides in the Caco-2 Cell Monolayer

The amounts of both glucuronides were measured in the AP and BL after acacetin was loaded from the AP side to the BL side or vice versa. The efflux rates were expressed as the amount of metabolites effluxed per min (nmol/min). The results are shown in Fig. 7. The excreted amounts of Aca-7-Glu were remarkably higher than those of Aca-5-Glu ($p < 0.05$) (Fig. 7a). After acacetin was loaded on the BL side, the efflux rates of Aca-5-Glu and Aca-7-Glu in the BL side were approximately 2.5- and 4- fold higher than those in the AP side ($p < 0.05$), respectively (Fig. 7a). This finding indicated that acacetin glucuronides were more likely transported toward the BL side. In Fig. 7b, the intracellular concentrations of Aca-5-Glu on the AP side to the BL side were significantly different from those on the BL side to the AP side ($p < 0.05$). Conversely, the intracellular concentrations of Aca-7-Glu on the AP side to the BL side vice versa did not significantly differ.

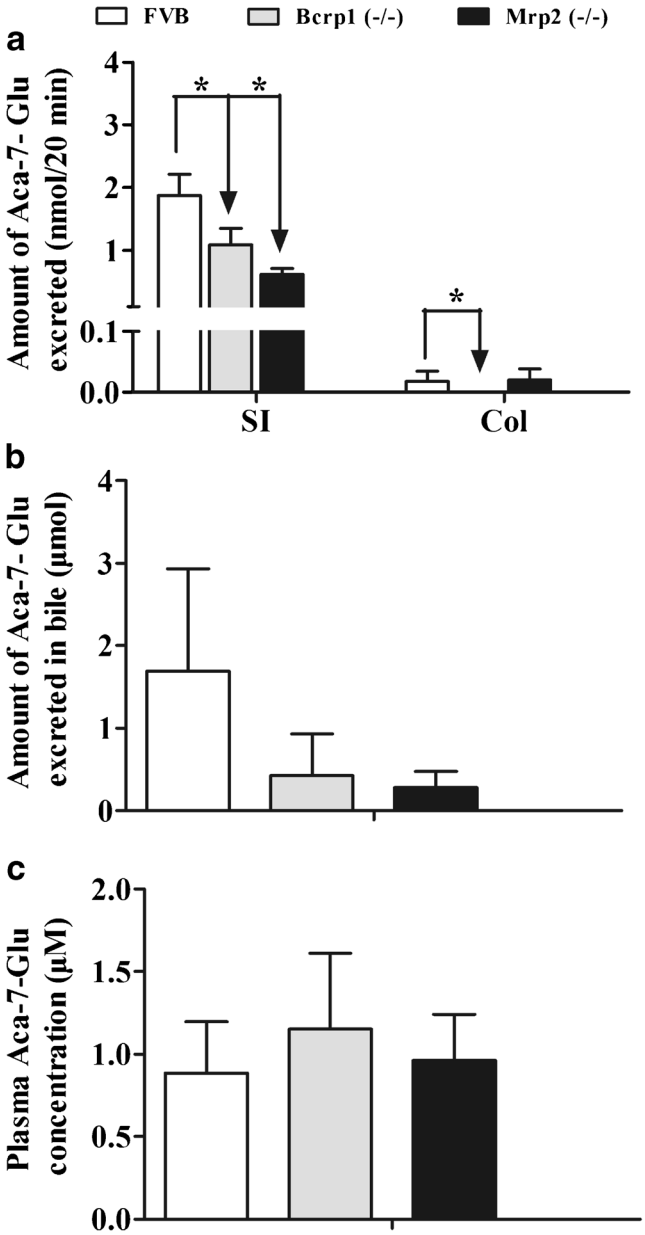

Fig. 4 Excretion of Aca-7-Glu in mouse intestinal perfusion. Panels (**a**), (**b**) and (**c**) represent excretion of Aca-7-Glu in intestine, bile and plasma in FVB, Bcrp1 (−/−) and Mrp2 (−/−) mice, respectively. In this experiment, two segments of intestine (small intestine and colon) were perfused simultaneously with 5 μM of acacetin at a flow rate of 0.25 mL/min. Aca-7-Glu excreted in lumen per 20 min were determined and normalized over 10 intestinal length. Plasma and bile samples were collected when the perfusion ended. The excreted amounts of Aca-7-Glu in bile and in plasma are expressed as micromole and micromole per litre, respectively, Each data point was the average of four determinations with the error bar representing the standard deviation of the mean. *$p < 0.05$.

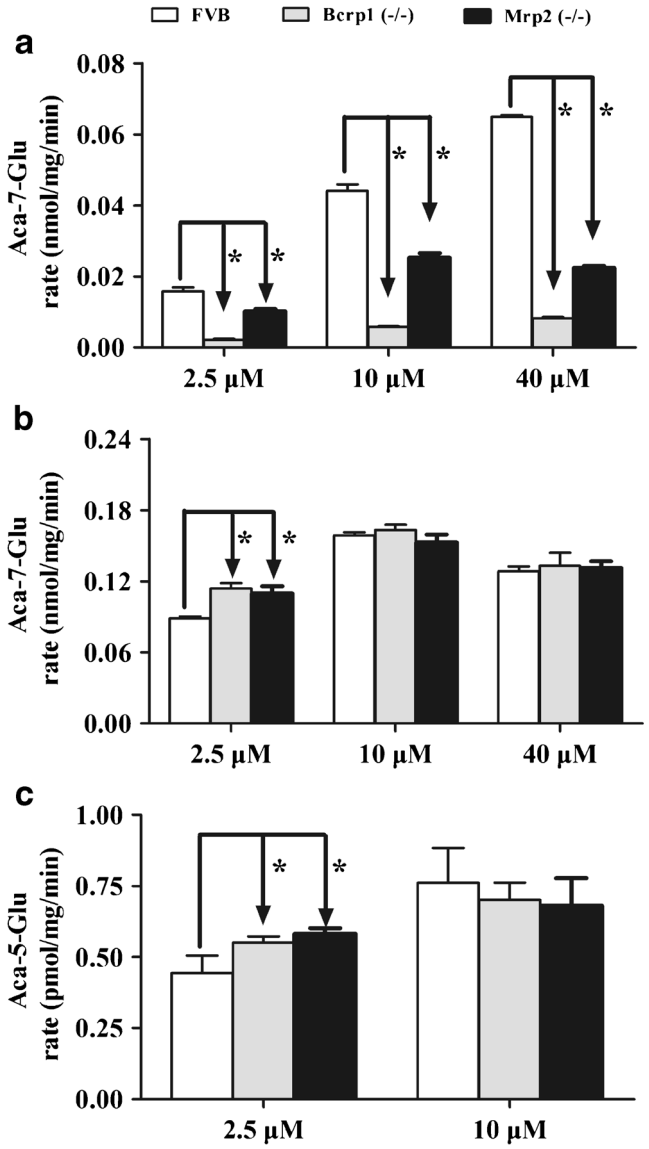

Fig. 5 Acacetin glucuronidation via hepatic and intestinal S9 fractions prepared from FVB, Bcrp1 (−/−) and Mrp2 (−/−) mice. Panels (**a**) and (**b**) show formation rates of Aca-7-Glu in liver and small intestine at 2.5, 10 and 40 μM, respectively, panel (**c**) shows formation rates of Aca- 5-Glu in intestine at 2.5 and 10 μM. The experiments were conducted at 37 °C for 30 min and the amounts of acacetin glucuronides were measured using UHPLC-MS/MS. Glucuronidation rates were expressed as nanomoles per min per milligram. Each bar represents the average of three determinations, and the error bars represent standard deviations ($n = 3$). *$p < 0.05$.

Effects of Transporter Inhibitors in the Caco-2 Cell Monolayer

The transporter inhibitors Ko143 (10 μM) and LTC4 (0.1 μM) were used to determine the roles of BCRP and MRP2 in the transport of acacetin glucuronides. Ko143 reduced the efflux rates of Aca-7-Glu in the BL to AP direction (BL to AP) and increased its intracellullar concentrations in the same direction (BL to AP) ($p < 0.05$) (Fig. 8b, c). However, Ko143 did not affect the efflux rates or intracellular concentrations of Aca-7-Glu in the AP to BL direction. Aca-5-Glu detected in both apical and basolateral compartment after either loading of acacetin was markedly lower in the presence of Ko143 than those in the control ($p < 0.05$) (Fig. 8e, f).

The intracellular concentrations of Aca-5-Glu were significantly increased in the BL to AP direction ($p < 0.05$) whereas

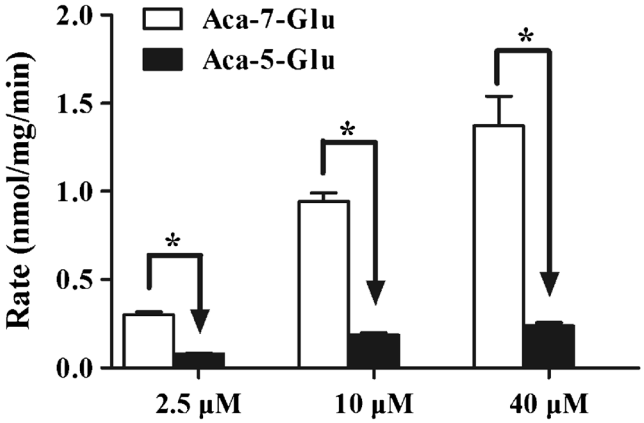

Fig. 6 Glucuronidation of acacetin at 2.5, 10 and 40 μM in Caco-2 cell lysate. The experiments were conducted at 37 °C for 30 min and the amounts of acacetin glucuronides were measured using UHPLC-MS/MS. Glucuronidation rates were expressed as nanomoles per min per milligram. Each bar represents the average of three determinations, and the error bars represent standard deviations ($n = 3$). *$p < 0.05$.

these concentrations did not significantly change in the opposite direction (Fig. 8g). The efflux rates of Aca-7-Glu and Aca-5-Glu in the BL-to-AP direction were reduced by LTC4 loaded on the AP side ($p < 0.05$) (Fig. 8b, f) but critical effects were not observed in the AP-to-BL direction. The intracellular concentrations of Aca-7-Glu and Aca-5-Glu were significantly increased by LTC4 regardless of the direction ($p < 0.05$) (Fig. 8c, g). Compared with that of the control, F_{met} of Aca-7-Glu and Aca-5-Glu were significantly reduced by Ko143 and LTC4 ($p < 0.05$) (Fig. 8d, h) in both directions.

DISCUSSION

In vitro glucuronidation metabolism and pharmacokinetics of acacetin have been reported. However, the bioavailability of acacetin, as well as the *in vivo* disposition characteristics of acacetin and its glucuronides are unclear. Our data clearly demonstrated that acacetin yielded poor oral bioavailability and the acacetin glucuronides, not acacetin, were more likely the main forms circulating in the blood. Our study also demonstrated that the pharmacokinetics and excretion of acacetin glucuronides could be markedly affected by modulating BCRP and MRP2.

Pharmacokinetic data in FVB mice suggested that acacetin was rapidly absorbed and eliminated after it was orally administered. Large amounts of acacetin glucuronides were found in plasma (Fig. 2). This result is consistent with our previous *in vitro* finding, which revealed that acacetin undergoes extensive metabolism. (17). The absolute bioavailability of acacetin in FVB mice is 1.3% (Fig. 2). The plasma $AUC_{0-\infty}$ values of acacetin glucuronides (Aca-7-Glu and Aca-5-Glu) in Bcrp1 (−/−) mice and Mrp2 (−/−) mice were significantly higher than those in FVB mice (Fig. 3). This

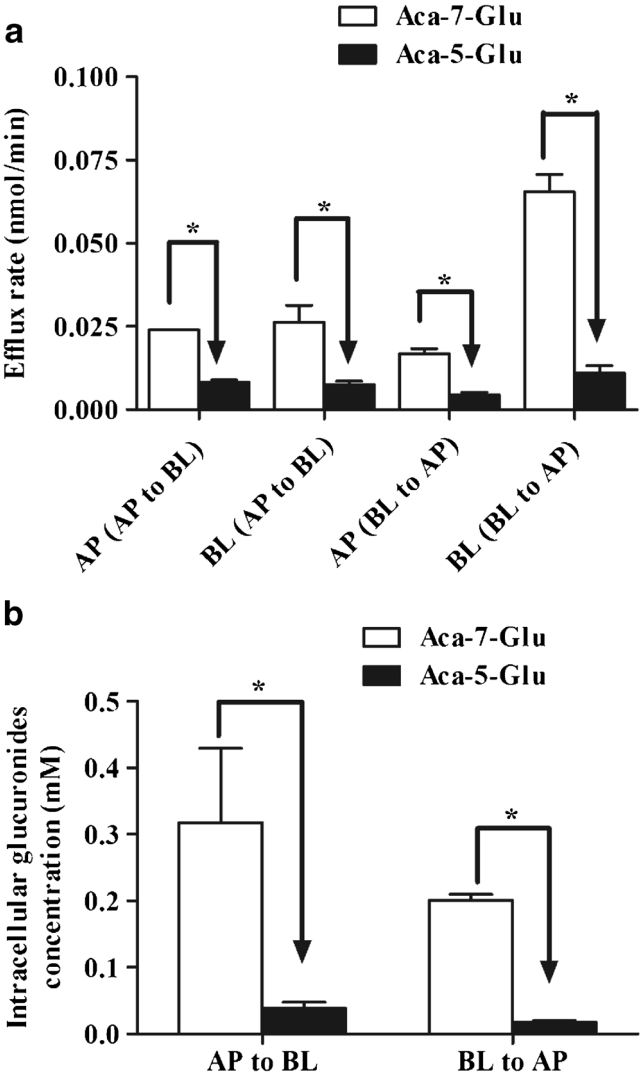

Fig. 7 Biodirectional efflux of acacetin glucuronides across Caco-2 cell monolayer. Efflux rates (**a**) of Aca-7-Glu and Aca-5-Glu and intracellular concentrations (**b**) of Aca-7-Glu and Aca-5-Glu from AP to BL and from BL to AP. After apical loading (AP to BL) or basolateral loading (BL to AP) of 10 μM acacetin, the amounts of Aca-7-Glu and Aca-5-Glu in the apical (AP) and basolateral (BL) sides were determined. The efflux rates and intracellular amounts of these glucuronides were calculated. Each data point was the average of three determinations with the error bar representing the standard deviation of the mean. *$p < 0.05$.

findings suggested that Bcrp and Mrp2 were probably involved in the efflux of Aca-7-Glu and Aca-5-Glu. Bcrp and Mrp2 were both located at apical membranes of intestine and liver, the knockout of these transporters could reduce the intestinal efflux and biliary excretion, when acacetin glucuronides functioned as the substrates of these transporters. Thus, more acacetin glucuronides could be excreted into the blood. By contrast, the efflux of acacetin glucuronides to the lumen was significantly reduced when Bcrp and Mrp2 were knocked out in intestinal perfusion experiments (Fig. 4a). Aca-7-Glu and Aca-5-Glu can be excreted to both apical side and basolateral side in the monolayer Caco-2 cells (Fig. 7a). Ko143 and LTC4

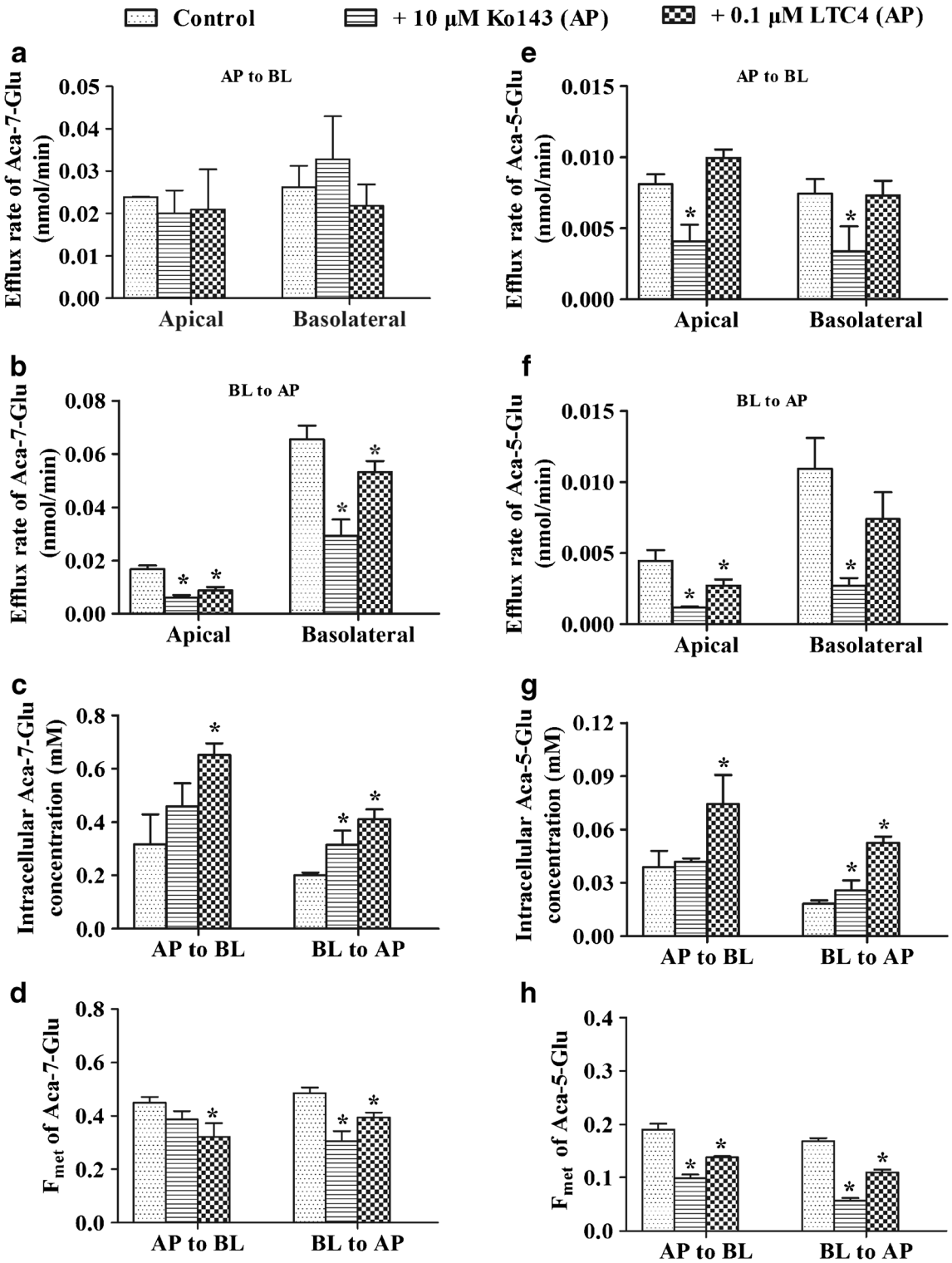

Fig. 8 Effects of Ko143 (an inhibitor of BCRP) and LTC4 (an inhibitor of MRP2) on the efflux rates, intracellular concentrations and F_{met} of Aca-7-Glu and Aca-5-Glu in Caco-2 cell model. Effects of Ko143 and LTC4 on efflux rates of Aca-7-Glu (**a**, **b**) and Aca-5-Glu (**e**, **f**). Effects of Ko143 and LTC4 on intracellular concentrations of Aca-7-Glu (**c**) and Aca-5-Glu (**g**). Effects of Ko143 and LTC4 on the F_{met} of Aca-7-Glu (**d**) and Aca-5-Glu (**h**). Acacetin (10 μM) was loaded at AP or BL side, Ko143 and LTC4 were loaded at AP side or no inhibitors were added, after then, the amounts of Aca-7-Glu and Aca-5-Glu in the AP and BL sides and their intracellular concentrations were determined. F_{met} was determined by comparing intracellular amounts of acacetin glucuronides and the intracellular amounts of acacetin aglycone. Each data point was the average of three determinations with the error bar representing the standard deviation of the mean. *$p < 0.05$.

significantly inhibited the efflux transportation of Aca-7-Glu and Aca-5-Glu to apical side (Fig. 8). These results are well correlated and provide strong evidence that BCRP and MRP2 are involved in the excretion of Aca-7-Glu and Aca-5-Glu.

BCRP, MRP2 and P-gp are highly expressed in the apical membrane of the liver and intestine, while MRP1 and MRP3 are expressed on the basolateral membrane. BCRP and MRPs function to pump out of drugs or metabolites with a high hydrophilicity (e.g., glucuronides and sulfates) (25,26). In contrast, the substrates of P-gp are lipophilic (27,28). In the current study, we systematically investigated the roles of apical efflux transporters in the efflux of acacetin glucuronides. Thus, BCRP and MRP2 were selected in this study. Moreover, we had evaluated the role of MRP3 in the transport of acacetin glucuronides using LTC4 added to basolateral compartment. LTC4 is used an effective inhibitors for MRPs in numerous literatures (20,29,30). When added to basolateral compartment, it significantly reduced the transport, efflux rates, and increased the intracellular concentrations of acacetin glucuronides ($p < 0.05$). Therefore, MRP3 possibly mediated the acacetin glucuronide transport. However, in this study, we aimed to determine apical efflux transporters involved in the excretion of acacetin glucuronides to apical membrance. Based on this fact, we evaluated the effects of BCRP and MRP2 on the excretion of acacetin glucuronides. Additionally, we also determined whether acacetin was involved in active transport. The efflux ratio is determined to be less than 1.5, implying that the cellular transport of acacetin was probably by passive diffusion.

Acacetin can be glucuronidated in the intestine and liver *in vivo*, as proved by the results obtained from the mouse intestinal perfusion (Fig. 4a) and large amounts of Aca-7-Glu found in the liver (Fig. 3d1). These findings are consistent with our previous study where acacetin is easily metabolized into Aca-7-Glu by hepatic and intestinal microsomes prepared from different animals (17). We also investigated the sulfation metabolism of acacetin in another study (manuscript under review). The results showed that the sulfation affinity of acacetin is rather weaker than glucuronidation *in vivo* or *in vitro*.

The difference in excretion rate between small intestine and colon is due to the different expression of UGT enzymes and efflux transporters (including BCRP and MRPs). UGT enzymes are abundantly expressed in small intestine but less in colon (31). Thus, the formation rate of acacetin glucuronides in small intestine is rather faster than that in the colon. Compared to colon, the expression of efflux transporters is more abundant in small intestine (32). Therefore, the remarkable difference of acacetin glucuronides excretion rates between small intestine and colon probably resulted from the difference of metabolism and efflux capabilities between small intestine and colon (Fig. 4a). In addition, efflux transporters (P-gp, BCRP and MRPs) are distributed extensively in human intestine, though differences of the expression of these efflux transporters exist in various intestinal segments (33). ABCB1 (P-gp) and ABCG2 (BCRP) are considerable more abundant in jejunum and ileum than in colon. While ABCC2 (MRP2) and ABCC3 (MRP3) show the highest expression level in colon (33).

Ko143 is thought to be an effective inhibitor of BCRP. However, at the concentration of 10 μM, this inhibitor might not be specific for BCRP as the enzyme activity could be also affected (34). Similarly, LTC4 is used to be an inhibitor for MRPs, other MRPs could be also influenced, since it probably diffuse into the cell and inhibit other MRPs on the basolateral side (35). Additionally, it was reported that LTC4 can be metabolized into LTD_4 and LTE_4 by cell surface proteases (36). It was also revealed that LTC4 remains stable within 60 min (>80% reversible) (35). These caveats should be noticed when LTC4 is selected as an inhibitor for a study. In addition, the present study found that the knockout of Bcrp and Mrp2 could reduce the glucuronidation activity in the liver but could increase this activity in the intestine (Fig. 5). Our previous study also demonstrated a decreased glucuronidation activity through Bcrp knockout (37). Moreover, Mrp2 and Mrp3 expression levels are not affected in Bcrp1 (−/−) mice. In Mrp2 (−/−) mice, Bcrp expression remains unchanged whereas Mrp3 expression increases (38). However, increase in Mrp3 in liver of Mrp2 (−/−) mice is not found in Chu's study (39). In our study, knockout mice were used to demonstrate the roles of efflux transporters in influencing the systemic exposure and excretion of acacetin glucuronides because efflux transporter knockout possibly affects glucuronidation activity or protein expression.

Caco-2 cell model and knockout mice model are combined to investigate the role of efflux transporters in this study. However, species differences in abundance and substrates for transporters should be noted. Caco-2 cells are derived from human colon carcinoma, this cell line efficiently expresses MRP2, MRP3, MRP4 and lower expression levels for BCRP (40,41). The efflux transporter expression in mouse liver, kidney, and intestine also includes Mrps, Bcrp (42). Nevertheless, the abundance and substrate specificity of transporters in knockout mice and Caco-2 cells can be quite different. For BCRP, they share 87% sequence homology and efflux identical substrates (43). The amino acid sequence identified in human MRP2 with its mouse ortholog is approximately 78% (44). These facts imply that the function of these transporters may differ markedly in substrate recognition. Despite extensive overlapping substrate specificity, noticeable differences in transport and modulation properties were revealed between human MRP2 and mouse Mrp2 (44). In the current study, the results obtained from the Caco-2 cells are well consistent with those from the pharmcokinetics and mouse intestinal perfusion. Hence, the current data have provided strong evidence that the disposition of acacetin glucuronides can be evidently altered by modulation of BCRP and MRP2.

CONCLUSIONS

In conclusion, acacetin exhibited poor bioavailability, and acacetin glucuronides, not acacetin, exsisted mostly in plasma after oral administration. Efflux transporters BCRP and MRP2 significantly altered the levels of acacetin glucuronides, as catalyzed by UGTs *in vivo*. Therefore, BCRP and MRP2 play a critical role in the disposition of acacetin glucuronides. Rapid glucuronidation metabolism and efflux by BCRP and MRP2 play an important role in the low bioavailability of acacetin.

ACKNOWLEDGMENTS AND DISCLOSURES

This work was supported by the grants of Key International Joint Research Project of National Natural Science Foundation of China (81120108025), Science and Technology Project of Guangzhou City (201509010004), and Guangdong Natural Science Foundation (2015AD030312012).

REFERENCES

1. Zhang L, Zuo Z, Lin G. Intestinal and hepatic glucuronidation of flavonoids. Mol Pharm. 2007;4(6):833–45.
2. Li W, Sun H, Zhang X, Wang H, Wu B. Efflux transport of chrysin and apigenin sulfates in HEK293 cells overexpressing SULT1A3: the role of multidrug resistance-associated protein 4 (MRP4/ABCC4). Biochem Pharmacol. 2015;98(1):203–14.
3. Siissalo S, Laine L, Tolonen A, Kaukonen AM, Finel M, Hirvonen J. Caco-2 cell monolayers as a tool to study simultaneous phase II metabolism and metabolite efflux of indomethacin, paracetamol and 1-naphthol. Int J Pharm. 2010;383(1–2):24–9.
4. Xu H, Kulkarni KH, Singh R, Yang Z, Wang SW, Tam VH, *et al.* Disposition of naringenin via glucuronidation pathway is affected by compensating efflux transporters of hydrophilic glucuronides. Mol Pharm. 2011;6(6):1703–15.
5. Jiang W, Hu M. Mutual interactions between flavonoids and enzymatic and transporter elements responsible for flavonoid disposition via phase II metabolic pathways. RSC Adv. 2012;2(21):7948–63.
6. Zhang X, Dong D, Wang H, Ma Z, Wang Y, Wu B. Stable knockdown of efflux transporters leads to reduced glucuronidation in UGT1A1-overexpressing HeLa cells: the evidence for glucuronidation-transport interplay. Mol Pharm. 2015;12(4):1268–78.
7. Sesink AL, Arts IC, de Boer VC, Breedveld P, Schellens JH, Hollman PC, *et al.* Breast cancer resistance protein (Bcrp1/Abcg2) limits net intestinal uptake of quercetin in rats by facilitating apical efflux of glucuronides. Mol Pharmacol. 2005;67(6):1999–2006.
8. Sakamoto S, Kusuhara H, Horie K, Takahashi K, Baba T, Ishizaki J, *et al.* Identification of the transporters involved in the hepatobiliary transport and intestinal efflux of methyl 1-(3,4-dimethoxyphenyl)-3-(3-ethylvaleryl)-4-hydroxy-6,7,8-trimethoxy-2-naphthoate (S-8921) glucuronide, a pharmacologically active metabolite of S-8. Drug Metab Dispos. 2008;36(8):1553–61.
9. Jaiswal S, Sharma A, Shukla M, Vaghasiya K, Rangaraj N, Lal J. Novel pre-clinical methodologies for pharmacokinetic drug-drug interaction studies: spotlight on "humanized" animal models. Drug Metab Rev. 2014;46(4):475–93.
10. Mamidi RNVS, Dallas S, Sensenhauser C, Lim HK, Scheers E, Verboven P, *et al. In vitro* and PBPK based assessment of drug-drug interaction potential of canagliflozin. Brit J Clin Pharmaco. 2016
11. Martinez-Vazquez M, Estrada-Reyes R, Martinez-Laurrabaquio A, Lopez-Rubalcava C, Heinze G. Neuropharmacological study of *Dracocephalum moldavica* L. (Lamiaceae) in mice: sedative effect and chemical analysis of an aqueous extract. J Ethnopharmacol. 2012;141(3):908–17.
12. Jiang L, Fang G, Zhang Y, Cao G, Wang S. Analysis of flavonoids in propolis and *Ginkgo biloba* by micellar electrokinetic capillary chromatography. J Agric Food Chem. 2008;56(24):11571–7.
13. Bi C, Dong X, Zhong X, Cai H, Wang D, Wang L. Acacetin protects mice from *Staphylococcus aureus* bloodstream infection by inhibiting the activity of sortase A. Molecules. 2016;21(10):1285.
14. Watanabe K, Kanno S, Tomizawa A, Yomogida S, Ishikawa M. Acacetin induces apoptosis in human T cell leukemia Jurkat cells via activation of a caspase cascade. Oncol Rep. 2012;27(1):204–9.
15. Liu H, Wang YJ, Yang L, Zhou M, Jin MW, Xiao GS, *et al.* Synthesis of a highly water-soluble acacetin prodrug for treating experimental atrial fibrillation in beagle dogs. Sci Rep-UK. 2016;6:25743.
16. Huang WC, Liou CJ. Dietary acacetin reduces airway hyperresponsiveness and eosinophil infiltration by modulating eotaxin-1 and Th2 cytokines in a mouse model of asthma. Evid-based Compl Alt. 2012;2012(5):910520.
17. Dai P, Luo F, Ying W, Jiang H, Wang L, Zhang G, *et al.* Species- and gender-dependent differences in the glucuronidation of a flavonoid glucoside and its aglycone determined using expressed UGT enzymes and microsomes. Biopharm Drug Dispos. 2015;36(9):622–35.
18. Li Q, Wang L, Dai P, Zeng X, Qi X, Zhu L, *et al.* A combined strategy of mass fragmentation, post-column cobalt complexation and shift in ultraviolet absorption spectra to determine the uridine 5′-diphospho-glucuronosyltransferase metabolism profiling of flavones after oral administration of a flavone mixture in rats. J Chromatogr A. 2015;1395:116–28.
19. Dai P, Zhu L, Luo F, Lu L, Li Q, Wang L, *et al.* Triple recycling processes impact systemic and local bioavailability of orally administered flavonoids. AAPS J. 2015;17(3):723–36.
20. Jeong EJ, Jia X, Hu M. Disposition of formononetin via enteric recycling: metabolism and excretion in mouse intestinal perfusion and Caco-2 cell models. Mol Pharm. 2005;2(4):319–28.
21. Tang L, Li Y, Chen WY, Zeng S, Dong LN, Peng XJ, *et al.* Breast cancer resistance protein-mediated efflux of luteolin glucuronides in HeLa cells overexpressing UDP-glucuronosyltransferase 1A9. Pharm Res. 2014;31(4):847–60.
22. Ye L, Lu L, Li Y, Zeng S, Yang X, Chen W, *et al.* Potential role of ATP-binding cassette transporters in the intestinal transport of rhein. Food Chem Toxicol. 2013;58(7):301–5.
23. Liu W, Feng Q, Li Y, Ye L, Hu M, Liu Z. Coupling of UDP-glucuronosyltransferases and multidrug resistance-associated proteins is responsible for the intestinal disposition and poor bioavailability of emodin. Toxicol Appl Pharmacol. 2012;265(3):316–24.
24. Tang L, Ye L, Singh R, Wu B, Lv C, Zhao J, *et al.* Use of glucuronidation fingerprinting to describe and predict mono- and dihydroxyflavone metabolism by recombinant UGT isoforms and human intestinal and liver microsomes. Mol Pharm. 2010;7(3):664–79.
25. Kawabata S, Oka M, Shiozawa K, Tsukamoto K, Nakatomi K, Soda H, *et al.* Breast cancer resistance protein directly confers SN-38 resistance of lung cancer cells. Biochem Bioph Res Co. 2001;280(5):1216–23.
26. Kalapos-Kovács B, Magda B, Jani M, Fekete Z, Szabó PT, Antal I, *et al.* Multiple ABC transporters efflux baicalin. Phytother Res. 2015;29(12):1987-90.

27. Wind NS, Holen I. Multidrug resistance in breast cancer: from *in vitro* models to clinical studies. Int J Breast Cancer. 2011;2011:967419.
28. Jeong EJ, Liu X, Jia X, Chen J, Hu M. Coupling of conjugating enzymes and efflux transporters: impact on bioavailability and drug interactions. Curr Drug Metab. 2005;6(5):455–68.
29. Grant CE, Gao M, Degorter MK, Cole SP, Deeley RG. Structural determinants of substrate specificity differences between human multidrug resistance protein (MRP) 1 (ABCC1) and MRP3 (ABCC3). Drug Metab Dispos. 2008;36(12):2571–81.
30. Hu M, Chen J, Lin H. Metabolism of flavonoids via enteric recycling: mechanistic studies of disposition of apigenin in the Caco-2 cell culture model. J Pharm Exp Ther. 2003;307(1):314–21.
31. Tang L, Feng Q, Zhao J, Dong L, Liu W, Yang C, *et al.* Involvement of UDP-glucuronosyltranferases and sulfotransferases in the liver and intestinal first-pass metabolism of seven flavones in C57 mice and humans *in vitro*. Food Chem Toxicol. 2012;50(5):1460–7.
32. Sai Y. Biochemical and molecular pharmacological aspects of transporters as determinants of drug disposition. Drug Metab Pharmacokinet. 2005;20(2):91–9.
33. Drozdzik M, Gröer C, Penski J, Lapczuk J, Ostrowski M, Lai Y, *et al.* Protein abundance of clinically relevant multidrug transporters along the entire length of the human intestine. Mol Pharm. 2014;11(10):3547–55.
34. Quan E, Wang H, Dong D, Zhang X, Wu B. Characterization of Chrysin Glucuronidation in UGT1A1-overexpressing HeLa cells: elucidating the transporters responsible for efflux of glucuronide. Drug Metabol Dispos. 2015;43(4):433–43.
35. Krilis S, Lewis RA, Corey EJ, Austen KF. Specific binding of leukotriene C4 to ileal segments and subcellular fractions of ileal smooth muscle cells. P Natl Acad Sci USA. 1984;81(14):4529–33.
36. Haeggström JZ, Funk CD. Lipoxygenase and leukotriene pathways: biochemistry, biology, and roles in disease. Chem Rev. 2011;111(10):5866–98.
37. Zheng L, Zhu L, Zhao M, Shi J, Li Y, Yu J, *et al. In Vivo* exposure of Kaempferol is driven by phase II metabolic enzymes and efflux transporters. AAPS J. 2016;18(5):1289–99.
38. Nezasa K, Tian X, Zamek-Gliszczynski MJ, Patel NJ, Raub TJ, Brouwer KL. Altered hepatobiliary disposition of 5 (and 6)-carboxy-2′,7′-dichlorofluorescein in Abcg2 (Bcrp1) and Abcc2 (Mrp2) knockout mice. Drug Metab Dispos. 2006;34(4):718–23.
39. Chu XY, Strauss JR, Mariano MA, Li J, Newton DJ, Cai X, *et al.* Characterization of mice lacking the multidrug resistance protein MRP2 (ABCC2). J Pharmacol Exp The. 2006;317(2):579–89.
40. Alnouti Y, Klaassen CD. Tissue distribution and ontogeny of sulfotransferase enzymes in mice. Toxicol Sci. 2006;93(2):242–55.
41. Prime-Chapman HM. Differential multidrug resistance-associated protein 1 through 6 isoform expression and function in human intestinal epithelial Caco-2 cells. J Pharmacol Exp Ther. 2004;311(2):476–84.
42. Chu X, Bleasby K, Evers R. Species differences in drug transporters and implications for translating preclinical findings to humans. Expert Opin Drug Met. 2013;9(3):237–52.
43. Natarajan K, Yi X, Nakanishi T, Beck WT, Bauer KS, Ross DD. Identification and characterization of the major alternative promoter regulating Bcrp1/Abcg2 expression in the mouse intestine. Biochim Biophys Acta. 2011;1809(7):295–305.
44. Zimmermann C, van de Wetering K, van de Steeg E, Wagenaar E, Vens C, Schinkel AH. Species-dependent transport and modulation properties of human and mouse multidrug resistance protein 2 (MRP2/Mrp2, ABCC2/Abcc2). Drug Metab Dispos 2008;36(4):631–40.